

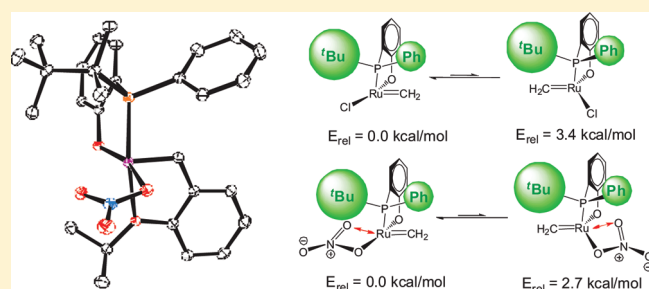
# Non-innocent Character of Oxyanions in Ruthenium Metathesis Catalysts

Marija Jović, Sebastian Torker, and Peter Chen\*

Laboratorium für Organische Chemie, Eidgenössische Technische Hochschule (ETH), Wolfgang-Pauli-Strasse 10, CH-8093 Zürich, Switzerland

Supporting Information

**ABSTRACT:** The synthesis, characterization, reactivity, and selectivity of six novel ruthenium metathesis catalysts containing oxyanions as ligands are described. A drop in chemoselectivity and/or reactivity in alternating ring-opening metathesis polymerization of norbornene and cyclooctene for catalysts with nitrate, acetate, and benzoate ligands (i.e., catalysts **7**, **8**, and **10a**) compared to the parent complex bearing chloride as a ligand (**5b**) is observed, while catalysts with trifluoroacetate, methylbenzoate, and triisopropylbenzoate ligands (i.e., catalysts **9**, **10b**, and **10c**) exhibit the expected activities and chemoselectivities. A model accounting for the aforementioned observations is based on a chelating effect of oxyanion ligands in these complexes and is supported by NMR data, crystal structures of the new complexes, and DFT calculations. Through comparison of selectivity and reactivity in copolymerizations with NMR and X-ray structures, we have uncovered correlations that serve as predictive tools for catalyst design.



## INTRODUCTION

Since the discovery of the first metathesis catalysts, olefin metathesis rapidly gained an important position in organic synthesis as well as in polymer chemistry.<sup>1–5</sup> This was achieved by the development of well-defined, highly active catalysts by optimizing the ligand sphere around the corresponding metal center.<sup>6–10</sup> For instance, replacement of one of the phosphines in first-generation Grubbs' catalyst (**1**) by N-heterocyclic carbenes (NHCs) resulted in second-generation Grubbs' catalyst (**2**), which exhibits enhanced reactivity by several orders of magnitude compared to the former (Chart 1).<sup>11,12</sup> Similarly, the introduction of the "Hoveyda-type unit",<sup>13,14</sup> i.e., the [(=CH-2-(2-PrOC<sub>6</sub>H<sub>4</sub>))] carbene ligand, resulted in olefin metathesis catalysts with increased stability and recyclability. Further variations and improvements of ligand sphere are numerous and have been published by many groups.<sup>4–17,21–44,46–51,57–59</sup>

Through mechanistic studies<sup>18–20</sup> in the field of ROMP by our group, and altering the ligand sphere around the ruthenium, the first example of a rationally designed ruthenium catalyst that can produce alternating copolymers was developed (**3**).<sup>21</sup> Further structural work and correlation of the structures to selectivity have produced a catalyst structure whose complete chemoselectivity in alternating copolymerization was demonstrated even at room temperature with modest ratios of cyclooctene to norbornene (**5a,b**).<sup>22–24</sup>

Subsequent replacement of the chloride anion in **5b** by various sulfonates (**11a–d**) of increasing steric bulk allowed us then to tune the *cis/trans* ratio of the produced copolymer, while leaving the chemoselectivity unchanged (**6a–d**).<sup>23</sup> However, despite the

possibility of steering the *cis/trans* ratio, a diminished reactivity as compared to the parent complex **5b** was observed.<sup>23</sup>

To guide further refinement of our catalyst system, we have discovered additional structural parameters that effect selectivity and reactivity and are presented through a series of complexes with carboxylate ligands (**8–10**), as well as the nitrate ligand (**7**). There have been reports in the literature<sup>25–39</sup> about replacement of the chloride ligands by other electron-withdrawing groups (Figure 1), although, in general, not too much attention has been dedicated to this topic. The reason might be that replacement of the halide has an effect on reactivity, although it is hard to predict whether it will be an increase or decrease.<sup>40–42</sup> Here we document the negative effect of a chelating oxyanion ligand on the rate and selectivity in alternating ring-opening metathesis polymerization (AROMP) and introduce NMR and crystallographic parameters that correlate with the degree to which the negative effects actually appear.

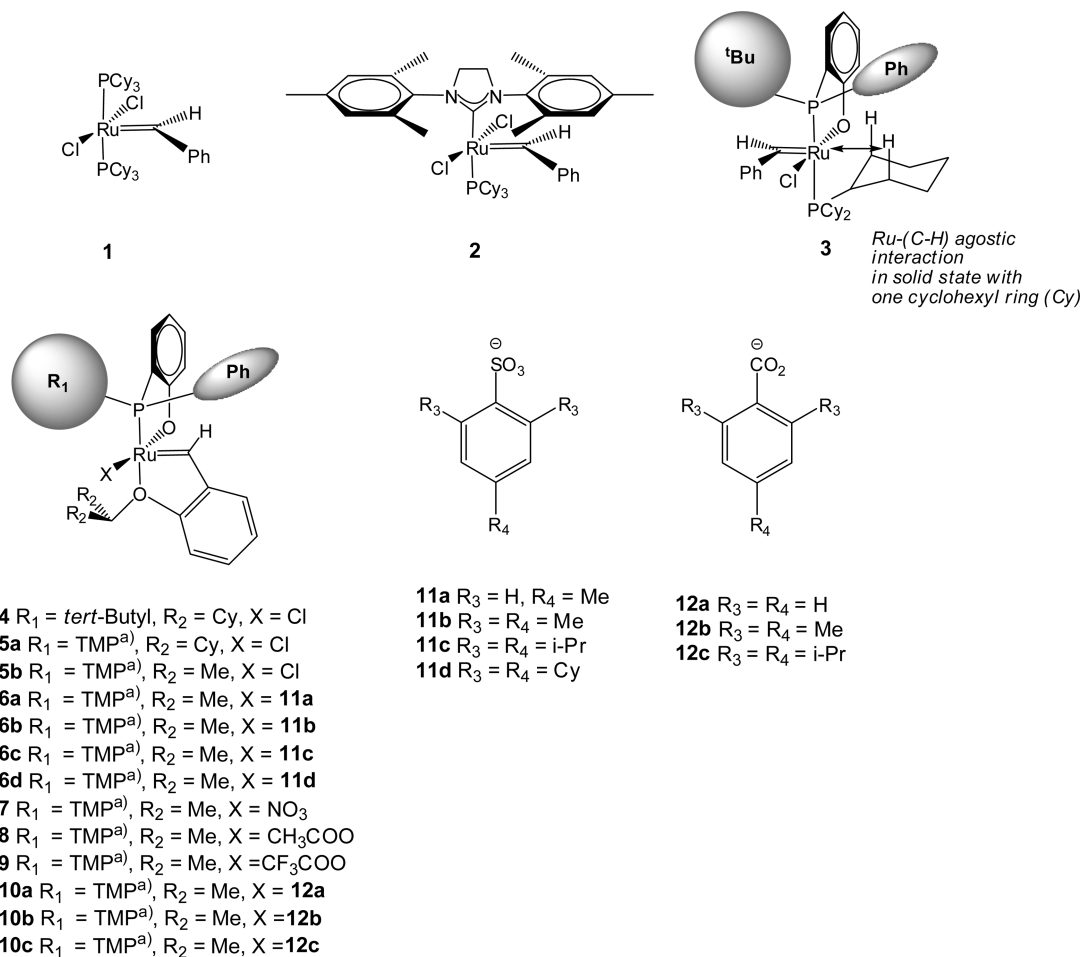
## EXPERIMENTAL SECTION

**General Remarks.** Unless otherwise stated, all manipulations were carried out under an argon atmosphere on a vacuum line using standard Schlenk techniques. The solvents were dried by distillation from the following drying agents prior to use and were transferred under N<sub>2</sub>: diethyl ether (Na/K), *n*-hexane (Na/K), CH<sub>2</sub>Cl<sub>2</sub> (CaH<sub>2</sub>). Flash chromatography was performed using Fluka silica gel 60, type 60752 (230–400 mesh). NMR measurements were either performed on 300

Received: February 9, 2011

Published: July 05, 2011

**Chart 1.** Grubbs' First-Generation Catalyst **1**, Grubbs' Second-Generation Catalyst **2**, Chemoselective AROMP Catalysts (prototype: **3**; previously reported optimized versions: **4**, **5a**, **5b**), Sulfonate Catalysts with Additional Stereocontrol (**6a–d**), Novel Nitrate Catalyst **7**, Acetate Catalyst **8**, Trifluoroacetate Catalyst **9**, and Benzoate Catalysts (**10a–c**)



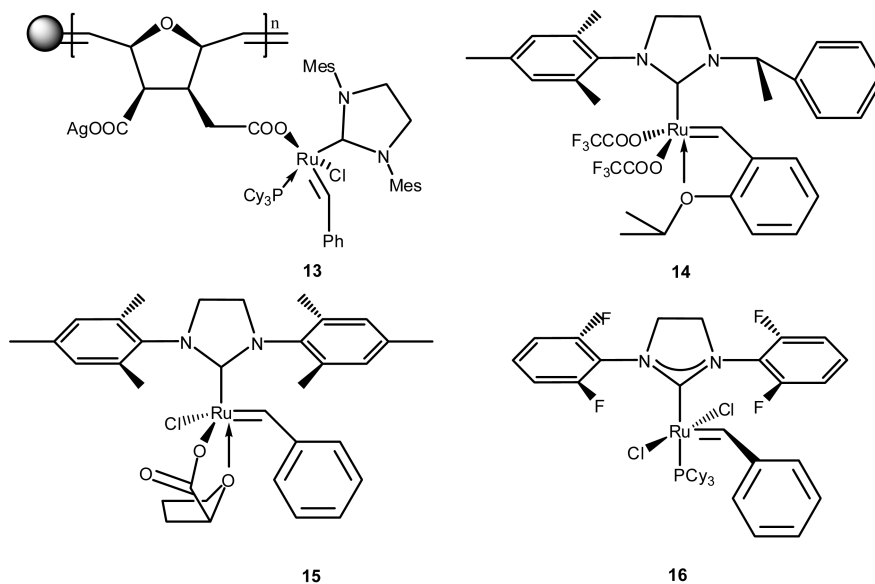
a) TMP = 1,1,2,2-Tetramethylpropyl-

( $^1\text{H}$ : 300 MHz,  $^{13}\text{C}$ : 75 MHz,  $^{31}\text{P}$ : 121 MHz) or 600 MHz instruments ( $^1\text{H}$ : 600 MHz,  $^{13}\text{C}$ : 150 Hz). Chemical shifts ( $\delta$ -values) are reported in ppm and calibrated with respect to the residual solvent signal for  $^1\text{H}$  and  $^{13}\text{C}$  NMR ( $\text{CD}_2\text{Cl}_2$ : 5.32 and 53.80 ppm;  $\text{CDCl}_3$ : 7.26 and 77.00 ppm). An 85% aqueous  $\text{H}_3\text{PO}_4$  solution is used as an external standard for  $^{31}\text{P}$  NMR. Coupling constants ( $J$ ) are given in Hz.  $^{13}\text{C}$  NMR and  $^{31}\text{P}$  NMR spectra were proton broad-band-decoupled. The multiplicities of peaks are denoted by the following abbreviations: s: singlet, d: doublet, dd: doublet of doublets, t: triplet, tm: triplet with an additional unresolved m, m: multiplet, br: broad. Elemental analyses were performed by the Microanalytical Laboratory of the Laboratorium für Organische Chemie, ETH-Zürich. Syntheses of complexes **5b** and **6a** have been reported previously.<sup>23,24</sup>

**General Polymerization Procedure.** A 150–200 mg amount of norbornene (NBE) was polymerized in the presence of 20 equiv of cyclooctene (COE) under argon. Prior to polymerization, the reaction volume was filled up to 20 mL with  $\text{CH}_2\text{Cl}_2$ . The catalyst (1:2000 with respect to NBE) was then added, and the reaction temperature kept at room temperature. The reaction was stopped by precipitation with 100 mL of MeOH after 40 min. The coagulated polymer was dried under high vacuum for 2 h and analyzed by NMR in  $\text{CDCl}_3$ . The NMR measurements were conducted with 30–40 mg of polymer left overnight in the NMR solvent.

**Synthesis of Nitrate Complex 7.** Catalyst **6a** (10 mg, 13.9  $\mu\text{mol}$ ) and tetrabutylammonium nitrate (4.7 mg, 15.3  $\mu\text{mol}$ ) in 2 mL of benzene were stirred for 2 h at room temperature. After filtration, the complex was purified by crystallization, affording complex **7** in 53% yield. Suitable crystals for X-ray analysis were obtained by vapor diffusion of  $\text{Et}_2\text{O}$  into a concentrated solution of the complex in  $\text{CH}_2\text{Cl}_2$ .

$^1\text{H}$  NMR (600 MHz,  $\text{CD}_2\text{Cl}_2$ ):  $\delta$  15.63 (d, 1H,  $\text{CH}(\text{=Ru})$ ,  $J_{\text{H,P}} = 9.3$  Hz), 8.29 (very br s, 2H,  $\text{Ar}(\text{P})\text{H}_{\text{ortho}}$ ), 7.90 (td, 1H,  $\text{Ar}(\text{PO})\text{H}$ ,  $J_{\text{H,H}} = 1.5$  and 7.9 Hz), 7.61 (tm, 1H,  $\text{Ar}(\text{O})\text{H}$ ,  $J_{\text{H,H}} = 7.8$  Hz), 7.57 (td, 1H,  $\text{Ar}(\text{P})\text{H}_{\text{para}}$ ,  $J_{\text{H,H}} = 1.3$  and 7.5 Hz), 7.49 (br s, 2H,  $\text{Ar}(\text{P})\text{H}_{\text{meta}}$ ), 7.15 (d, 1H,  $\text{Ar}(\text{O})\text{H}$ ,  $J_{\text{H,H}} = 8.5$  Hz), 7.11 (tm, 1H,  $\text{Ar}(\text{PO})\text{H}$ ,  $J_{\text{H,H}} = 7.7$  Hz), 7.03 (td, 1H,  $\text{Ar}(\text{O})\text{H}$ ,  $J_{\text{H,H}} = 7.6$  and 1.7 Hz), 6.98 (td, 1H,  $\text{Ar}(\text{O})\text{H}$ ,  $J_{\text{H,H}} = 7.4$  and 0.8 Hz), 6.73 (tm, 1H,  $\text{Ar}(\text{PO})\text{H}$ ,  $J_{\text{H,H}} = 7.4$  Hz), 6.62 (ddd, 1H,  $\text{Ar}(\text{PO})\text{H}$ ,  $J_{\text{H,H}} = 8.4$ , 4.4, and 1.0 Hz), 5.25 (m, 1H,  $\text{CH}(\text{isopropoxy})$ ), 1.76 (d, 3H,  $\text{CH}_3(\text{isopropoxy})$ ,  $J_{\text{H,H}} = 6.3$  Hz), 1.60 (d, 3H,  $\text{CH}_3(\text{isopropoxy})$ ,  $J_{\text{H,H}} = 6.2$  Hz), 1.17 (d, 3H,  $\text{CH}_3(\text{TMP})$ ,  $J_{\text{H,P}} = 18.3$  Hz), 1.10 (d, 3H,  $\text{CH}_3(\text{TMP})$ ,  $J_{\text{H,P}} = 13.6$  Hz), 0.96 (s, 9H,  $\textit{tert}$ -butyl(TMP)).  $^{13}\text{C}$  NMR (150 MHz,  $\text{CD}_2\text{Cl}_2$ ):  $\delta$  295.88 (dd, 1C,  $\text{C}(\text{=Ru})$ ,  $J_{\text{C,P}} = 35.4$  and 13.5 Hz), 179.55 (d, 1C,  $\text{C}_{\text{Ar}(\text{PO})}(\text{ORu})$ ,  $J_{\text{C,P}} = 14.0$  Hz), 156.33 (s, 1C,  $\text{C}_{\text{Ar}(\text{O})}(\text{OR})$ ), 144.18 (s, 1C,  $\text{C}_{\text{Ar}(\text{O})}(\text{CH}=\text{Ru})$ ),  $\sim$ 136.3 and 132.8 (2 very br s almost in the baseline, 2C,  $\text{C}_{\text{Ar}(\text{P})}(\text{ortho})$ ), 133.72 (s, 1C,  $\text{C}_{\text{Ar}(\text{PO})}(\text{H})$ ), 132.46 (d, 1C,  $\text{C}_{\text{Ar}(\text{PO})}(\text{H})$ ,  $J_{\text{C,P}} = 1.7$  Hz), 131.31 (d, 1C,  $\text{C}_{\text{Ar}(\text{P})}(\text{ipso})$ ,  $J_{\text{C,P}} = 46.8$  Hz), 130.62 (d, 1C,  $\text{C}_{\text{Ar}(\text{P})}(\text{para})$ ,  $J_{\text{C,P}} = 2.3$  Hz), 130.40 (s, 1C,



Cy = cyclohexyl; Mes = 2,4,6-trimethylphenyl

**Figure 1.** Examples of ruthenium metathesis catalysts with carboxylate ligands by Buchmeiser (13, 2003; 14, 2009)<sup>25,32</sup> and Grubbs (15, 2008)<sup>39</sup> and a catalyst with a potential F–Ru interaction by Grubbs (16, 2006).<sup>36</sup>

$C_{Ar(O)}(H)$ , 128.37 (br s, 2C,  $C_{Ar(P)}$ (meta)), 123.86 (s, 1C,  $C_{Ar(O)}(H)$ ), 123.17 (s, 1C,  $C_{Ar(O)}(H)$ ), 119.63 (d, 1C,  $C_{Ar(PO)}(PRu)$ ),  $J_{C,P} = 42.9$  Hz), 119.20 (d, 1C,  $C_{Ar(PO)}(H)$ ),  $J_{C,P} = 9.9$  Hz), 117.43 (d, 1C,  $C_{Ar(PO)}(H)$ ),  $J_{C,P} = 6.5$  Hz), 114.12 (s, 1C,  $C_{Ar(O)}(H)$ ), 77.97 (s, 1C,  $C_{isopropoxy}$ ), 46.80 (d, 1C,  $C_{TMP}$ ),  $J_{C,P} = 23.7$  Hz), 38.45 (d, 1C,  $C_{TMP}$ ),  $J_{C,P} = 2.6$  Hz), 27.78 (d, 3C,  $C_{TMP}$ ),  $J_{C,P} = 4.9$  Hz), 22.83 (d, 1C,  $C_{TMP}$ ),  $J_{C,P} = 1.3$  Hz), 21.34 (s, 1C,  $C_{isopropoxy}$ ), 21.29 (d, 1C,  $C_{TMP}$ ),  $J_{C,P} = 7.2$  Hz), 21.20 (s, 1C,  $C_{isopropoxy}$ ).  $^{31}P$  NMR (121 MHz,  $CD_2Cl_2$ ):  $\delta$  78.38 (s). No elemental analysis was obtained due to traces of the tetrabutylammonium salt in the sample.

**Synthesis of Acetate Complex 8.** Catalyst 6a (10 mg, 13.9  $\mu$ mol) and ammonium acetate (1.2 mg, 15.3  $\mu$ mol) in 2 mL of benzene were stirred for 2 h at room temperature. The complex was filtered and used without further purification.

$^1H$  NMR (600 MHz,  $CD_2Cl_2$ ):  $\delta$  15.42 (d, 1H, CH(=Ru),  $J_{H,P} = 9.4$  Hz), 8.15 (very br s, 2H, Ar(P)H<sub>ortho</sub>), 7.89 (td, 1H, Ar(PO)H,  $J_{H,H} = 7.8$ , 1.5 Hz), 7.54 (tm, 1H, Ar(O)H,  $J_{H,H} = 7.2$  Hz), 7.51 (td, 1H, Ar(P)H<sub>para</sub>,  $J_{H,H} = 8.3$ , 1.3 Hz), 7.45 (br s, 2H, Ar(P)H<sub>meta</sub>), 7.09 (d, 1H, Ar(O)H,  $J_{H,H} = 8.4$  Hz), 7.05 (td, 1H, Ar(PO)H,  $J_{H,H} = 8.4$ , 7.0 Hz), 6.99 (dd, 1H, Ar(O)H,  $J_{H,H} = 7.6$ , 1.7 Hz), 6.92 (td, 1H, Ar(O)H,  $J_{H,H} = 7.4$ , 0.8 Hz), 6.66 (tm, 1H, Ar(PO)H,  $J_{H,H} = 7.0$  Hz), 6.55 (ddd, 1H, Ar(PO)H,  $J_{H,H} = 8.4$ , 4.4, 0.9 Hz), 5.17 (m, 1H, CH(isopropoxy)), 1.98 (s, 3H, CH<sub>3</sub>(acetate ligand)), 1.77 (d, 3H, CH<sub>3</sub>(isopropoxy)),  $J_{H,H} = 6.3$  Hz), 1.59 (d, 3H, CH<sub>3</sub>(isopropoxy)),  $J_{H,H} = 6.2$  Hz), 1.16 (d, 3H, CH<sub>3</sub>(TMP)),  $J_{H,P} = 17.8$  Hz), 1.08 (d, 3H, CH<sub>3</sub>(TMP)),  $J_{H,P} = 13.4$  Hz), 0.95 (s, 9H, *tert*-butyl(TMP)).  $^{13}C$  NMR (150 MHz,  $CD_2Cl_2$ ):  $\delta$  289.27 (d, 1C, C(=Ru)),  $J_{C,P} = 23.9$  Hz), 183.31 (s, 1C, COO, acetate ligand), 180.08 (d, 1C,  $C_{Ar(PO)}(ORu)$ ),  $J_{C,P} = 14.3$  Hz), 156.13 (s, 1C,  $C_{Ar(O)}(OR)$ ), 144.20 (s, 1C,  $C_{Ar(O)}(CH=Ru)$ ),  $\sim$ 136.3 and 131.5 (2 very br s almost in the baseline, 2C,  $C_{Ar(P)}$ (ortho)), 133.78 (s, 1C,  $C_{Ar(PO)}(H)$ ), 132.61 (d, 1C,  $C_{Ar(P)}$ (ipso)),  $J_{C,P} = 45.6$  Hz), 132.26 (d, 1C,  $C_{Ar(PO)}(H)$ ),  $J_{C,P} = 1.5$  Hz), 130.39 (d, 1C,  $C_{Ar(P)}$ (para)),  $J_{C,P} = 2.2$  Hz), 129.00 (s, 1C,  $C_{Ar(O)}(H)$ ), 128.16 (br s, 2C,  $C_{Ar(P)}$ (meta)), 123.82 (s, 1C,  $C_{Ar(O)}(H)$ ), 122.84 (s, 1C,  $C_{Ar(O)}(H)$ ), 121.02 (d, 1C,  $C_{Ar(PO)}(PRu)$ ),  $J_{C,P} = 42.2$  Hz), 119.24 (d, 1C,  $C_{Ar(PO)}(H)$ ),  $J_{C,P} = 9.8$  Hz), 116.71 (d, 1C,  $C_{Ar(PO)}(H)$ ),  $J_{C,P} = 6.4$  Hz), 113.95 (s, 1C,  $C_{Ar(O)}(H)$ ), 77.73 (s, 1C,  $C_{isopropoxy}$ ), 47.00 (d, 1C,  $C_{TMP}$ ),  $J_{C,P} = 23.6$  Hz), 38.48 (d, 1C,  $C_{TMP}$ ),  $J_{C,P} = 2.7$  Hz), 30.26 (s, 1C, CH<sub>3</sub>, acetate ligand), 28.16 (d, 3C,  $C_{TMP}$ ,

$J_{C,P} = 4.9$  Hz), 23.87 (s, 1C,  $C_{isopropoxy}$ ), 22.98 (s, 1C,  $C_{isopropoxy}$ ), 21.67 (d, 1C,  $C_{TMP}$ ),  $J_{C,P} = 7.2$  Hz), 21.62 (d, 1C,  $C_{TMP}$ ),  $J_{C,P} = 2.9$  Hz).  $^{31}P$  NMR (121 MHz,  $CD_2Cl_2$ ):  $\delta$  78.97 (s). HRMS (ESI+): calcd for  $C_{31}H_{39}NaO_4PRu$  [ $M + Na^+$ ] 631.1530, found 631.1515. No elemental analysis was obtained due to partial decomposition of the complex.

**Synthesis of Trifluoroacetate Complex 9.** Catalyst 5b (10 mg, 13.9  $\mu$ mol) and silver trifluoroacetate (2.5 mg, 15.3  $\mu$ mol) in 2 mL of  $CH_2Cl_2$  were stirred for 2 h at room temperature. After filtration, the complex was purified by crystallization, affording complex 9 in 40% yield. Suitable crystals for X-ray analysis were obtained by evaporation of  $Et_2O$  from a solution of the complex in  $Et_2O$  and hexane ( $Et_2O$ /hexane, 0.3 mL:0.3 mL) into hexane (0.1 mL in the outer flask, setup similar to vapor diffusion).

$^1H$  NMR (600 MHz,  $CD_2Cl_2$ ):  $\delta$  16.29 (d, 1H, CH(=Ru),  $J_{H,P} = 7.8$  Hz), 8.05 (br s, 2H, Ar(P)H<sub>ortho</sub>), 7.86 (td, 1H, Ar(PO)H,  $J_{H,H} = 7.7$ , 1.5 Hz), 7.60 (tm, 1H, Ar(O)H,  $J_{H,H} = 5.2$  Hz), 7.59 (td, 1H, Ar(P)H<sub>para</sub>,  $J_{H,H} = 8.1$ , 1.6 Hz), 7.55 (tm, 2H, Ar(P)H<sub>meta</sub>),  $J_{H,H} = 7.0$  Hz), 7.25 (dd, 1H, Ar(O)H,  $J_{H,H} = 7.6$ , 1.6 Hz), 7.13 (tm, 2H, Ar(O)H,  $J_{H,H} = 7.8$  Hz), 7.04 (td, 1H, Ar(PO)H,  $J_{H,H} = 7.5$ , 0.8 Hz), 6.76 (tm, 1H, Ar(PO)H,  $J_{H,H} = 7.8$  Hz), 6.65 (ddd, 1H, Ar(PO)H,  $J_{H,H} = 8.4$ , 4.4, and 1.0 Hz), 5.25 (m, 1H, CH<sub>3</sub>(isopropoxy)), 1.76 (d, 3H, CH(isopropoxy)),  $J_{H,H} = 6.1$  Hz), 1.63 (d, 3H, CH(isopropoxy)),  $J_{H,H} = 6.1$  Hz), 1.25 (d, 3H, CH<sub>3</sub>(TMP)),  $J_{H,P} = 12.1$  Hz), 1.23 (s, 9H, *tert*-butyl(TMP)), 1.08 (d, 3H, CH<sub>3</sub>(TMP)),  $J_{H,P} = 17.2$  Hz).  $^{13}C$  NMR (150 MHz,  $CD_2Cl_2$ ):  $\delta$  294.86 (dd, 1C, C(=Ru)),  $J_{C,P} = 18.0$ , 12.9 Hz), 178.78 (d, 1C,  $C_{Ar(PO)}(ORu)$ ),  $J_{C,P} = 14.3$  Hz), 161.02 (q, 1C, CF<sub>3</sub>,  $J_{C,F} = 36.4$  Hz), 155.31 (s, 1C,  $C_{Ar(O)}(OR)$ ), 143.63 (s, 1C,  $C_{Ar(O)}(CH=Ru)$ ),  $\sim$ 136.3 and 133.8 (2 very br s almost in the baseline, 2C,  $C_{Ar(P)}$ (ortho)), 133.60 (s, 1C,  $C_{Ar(PO)}(H)$ ), 132.97 (d, 1C,  $C_{Ar(PO)}(H)$ ),  $J_{C,P} = 1.6$  Hz), 131.16 (d, 1C,  $C_{Ar(P)}$ (para)),  $J_{C,P} = 2.4$  Hz), 130.26 (s, 1C,  $C_{Ar(O)}(H)$ ), 128.67 (d, 2C,  $C_{Ar(P)}$ (meta),  $J_{C,P} = 10.2$  Hz), 126.64 (d, 1C,  $C_{Ar(P)}$ (ipso)),  $J_{C,P} = 48.6$  Hz), 123.71 (s, 1C,  $C_{Ar(O)}(H)$ ), 123.07 (s, 1C,  $C_{Ar(O)}(H)$ ), 119.81 (d, 1C,  $C_{Ar(PO)}(H)$ ),  $J_{C,P} = 10.1$  Hz), 119.49 (d, 1C,  $C_{Ar(PO)}(PRu)$ ),  $J_{C,P} = 43.5$  Hz), 118.06 (d, 1C,  $C_{Ar(PO)}(H)$ ),  $J_{C,P} = 6.4$  Hz), 116.39 (br s, 1C, COO), 113.25 (s, 1C,  $C_{Ar(O)}(H)$ ), 75.19 (s, 1C,  $C_{isopropoxy}$ ), 47.61 (d, 1C,  $C_{TMP}$ ),  $J_{C,P} = 24.3$  Hz), 37.48 (d, 1C,  $C_{TMP}$ ),  $J_{C,P} = 5.2$  Hz), 29.03 (d, 3C,  $C_{TMP}$ ),  $J_{C,P} = 5.6$

Hz), 22.26 (s, 1C, C<sub>isopropoxy</sub>), 21.93 (s, 1C, C<sub>isopropoxy</sub>), 20.64 (d, 1C, C<sub>TMP</sub>, J<sub>C,P</sub> = 12.9 Hz), 20.60 (d, 1C, C<sub>TMP</sub>, J<sub>C,P</sub> = 7.0 Hz). <sup>31</sup>P NMR (121 MHz, CD<sub>2</sub>Cl<sub>2</sub>): δ 81.61 (s). Anal. Calcd (%) for C<sub>31</sub>H<sub>36</sub>O<sub>4</sub>FRu (661.66 g/mol): C 56.27, H 5.48. Found: C 56.15, H 5.56.

**Synthesis of Benzoate Complex 10a.** Catalyst **6a** (10 mg, 13.9 μmol) and sodium benzoate (2.2 mg, 15.3 μmol) in 2 mL of CH<sub>2</sub>Cl<sub>2</sub> were stirred for 2 h at room temperature. After filtration, the complex was purified by crystallization, affording complex **10a** in 60% yield. Suitable crystals for X-ray analysis were obtained by evaporation of Et<sub>2</sub>O from a solution of the complex in Et<sub>2</sub>O and pentane (Et<sub>2</sub>O/pentane, 0.3 mL:0.3 mL) into pentane (0.1 mL in the outer flask, setup similar to vapor diffusion).

<sup>1</sup>H NMR (600 MHz, CD<sub>2</sub>Cl<sub>2</sub>): δ 15.68 (d, 1H, CH(=Ru), J<sub>H,P</sub> = 9.1 Hz), 8.05 (very br s, 2H, Ar(P)H<sub>ortho</sub>), 8.04–8.02 (m, 1H, CH (benzoate ligand)), 8.02 (t, 1H, CH (benzoate ligand), J<sub>H,H</sub> = 1.7 Hz), 7.92 (td, 1H, Ar(PO)H, J<sub>H,H</sub> = 7.8, 1.5 Hz), 7.57–7.55 (m, 1H, Ar(O)H), 7.53 (td, 1H, Ar(P)H<sub>para</sub>, J<sub>H,H</sub> = 6.9, 1.7 Hz), 7.51 (br s, 2H, Ar(P)H<sub>meta</sub>), 7.47–7.43 (m, 1H, CH (benzoate ligand)), 7.39 (tt, 2H, CH (benzoate ligand), J<sub>H,H</sub> = 6.7, 1.3 Hz), 7.10 (ddd, 2H, Ar(O)H, J<sub>H,H</sub> = 8.2, 4.4, 1.5 Hz), 7.07 (d, 1H, Ar(O)H, J<sub>H,H</sub> = 8.4 Hz), 6.97 (td, 1H, Ar(PO)H, J<sub>H,H</sub> = 7.5, 0.8 Hz), 6.70 (tm, 1H, Ar(PO)H, J<sub>H,H</sub> = 8.1 Hz), 6.62 (ddd, 1H, Ar(PO)H, J<sub>H,H</sub> = 8.4, 4.4, 0.9 Hz), 5.18 (m, 1H, CH(isopropoxy)), 1.85 (d, 3H, CH<sub>3</sub>(isopropoxy), J<sub>H,H</sub> = 6.3 Hz), 1.46 (d, 3H, CH<sub>3</sub>(isopropoxy), J<sub>H,H</sub> = 6.2 Hz), 1.10 (d, 3H, CH<sub>3</sub>(TMP), J<sub>H,P</sub> = 13.0 Hz), 1.08 (d, 3H, CH<sub>3</sub>(TMP), J<sub>H,P</sub> = 17.5 Hz), 1.03 (s, 9H, *tert*-butyl(TMP)). <sup>13</sup>C NMR (150 MHz, CD<sub>2</sub>Cl<sub>2</sub>): δ 289.83 (dd, 1C, C(=Ru), J<sub>C,P</sub> = 37.7, 13.6 Hz), 179.94 (d, 1C, C<sub>Ar(PO)</sub>(ORu), J<sub>C,P</sub> = 14.2 Hz), 176.33 (s, 1C, COO (benzoate ligand)), 155.99 (s, 1C, C<sub>Ar(O)</sub>(OR)), 144.11 (s, 1C, C<sub>Ar(O)</sub>(CH=Ru)), ~136.3 and 132.8 (2 very br s almost in the baseline, 2C, C<sub>Ar(P)</sub>(ortho)), 134.56 (s, 1C, CCOO (benzoate ligand)), 133.79 (s, 1C, C<sub>Ar(PO)</sub>(H)), 132.40 (d, 1C, C<sub>Ar(PO)</sub>(H), J<sub>C,P</sub> = 1.4 Hz), 131.62 (s, 1C, C<sub>para</sub> (benzoate ligand)), 131.33 (d, 1C, C<sub>Ar(P)</sub>(ipso), J<sub>C,P</sub> = 46.8 Hz), 130.56 (d, 1C, C<sub>Ar(P)</sub>(para), J<sub>C,P</sub> = 2.2 Hz), 129.56 (s, 2C, C<sub>ortho</sub> (benzoate ligand)), 129.16 (s, 1C, C<sub>Ar(O)</sub>(H)), 128.48 (s, 2C, C<sub>meta</sub> (benzoate ligand)), 128.31 (br d, 2C, C<sub>Ar(P)</sub>(meta), J = 9.4 Hz), 123.77 (s, 1C, C<sub>Ar(O)</sub>(H)), 122.97 (s, 1C, C<sub>Ar(O)</sub>(H)), 120.87 (d, C<sub>Ar(PO)</sub>(PRu), J<sub>C,P</sub> = 42.3 Hz), 119.39 (d, 1C, C<sub>Ar(PO)</sub>(PRu), J<sub>C,P</sub> = 9.9 Hz), 116.96 (d, 1C, C<sub>Ar(PO)</sub>(H), J<sub>C,P</sub> = 6.4 Hz), 113.80 (s, 1C, C<sub>Ar(O)</sub>(H)), 77.13 (s, 1C, C<sub>isopropoxy</sub>), 47.15 (d, 1C, C<sub>TMP</sub>, J<sub>C,P</sub> = 23.6 Hz), 38.30 (d, 1C, C<sub>TMP</sub>, J<sub>C,P</sub> = 3.2 Hz), 28.43 (d, 3C, C<sub>TMP</sub>, J<sub>C,P</sub> = 5.0 Hz), 22.54 (d, 1C, C<sub>TMP</sub>, J<sub>C,P</sub> = 1.5 Hz), 21.77 (s, 1C, C<sub>isopropoxy</sub>), 21.63 (s, 1C, C<sub>isopropoxy</sub>), 21.60 (d, 1C, C<sub>TMP</sub>, J<sub>C,P</sub> = 8.4 Hz). <sup>31</sup>P NMR (121 MHz, CD<sub>2</sub>Cl<sub>2</sub>): δ 79.47 (s). Anal. Calcd (%) for C<sub>36</sub>H<sub>41</sub>O<sub>4</sub>PRu (669.76 g/mol): C 64.56, H 6.17. Found: C 64.27, H 6.20.

**Synthesis of Trimethylbenzoate Complex 10b.** Catalyst **6a** (10 mg, 13.9 μmol) and sodium 2,4,6-trimethylbenzoate (2.8 mg, 15.3 μmol) in 2 mL of CH<sub>2</sub>Cl<sub>2</sub> were stirred for 2 h at room temperature. After filtration, the complex was purified by crystallization, affording complex **10a** in 42% yield. Suitable crystals for X-ray analysis were obtained by evaporation of Et<sub>2</sub>O from a solution of the complex in Et<sub>2</sub>O and pentane (Et<sub>2</sub>O/pentane, 0.3 mL:0.3 mL) into pentane (0.1 mL in the outer flask, setup similar to vapor diffusion).

<sup>1</sup>H NMR (600 MHz, CD<sub>2</sub>Cl<sub>2</sub>): δ 15.84 (d, 1H, CH(=Ru), J<sub>H,P</sub> = 8.8 Hz), 8.19 (br s, 2H, Ar(P)H<sub>ortho</sub>), 7.92 (td, 1H, Ar(PO)H, J<sub>H,H</sub> = 7.7, 1.5 Hz), 7.57–7.54 (m, 2H, Ar(O)H), 7.53 (td, 1H, Ar(P)H<sub>para</sub>, J<sub>H,H</sub> = 6.9, 1.7 Hz), 7.50 (br t, 2H, Ar(P)H<sub>meta</sub>, J<sub>H,H</sub> = 6.7 Hz), 7.15 (dd, 1H, Ar(O)H, J<sub>H,H</sub> = 7.6, 1.6 Hz), 7.12 (d, 1H, Ar(O)H, J<sub>H,H</sub> = 8.4 Hz), 7.12–7.09 (m, 1H, Ar(O)H), 6.98 (td, 1H, Ar(PO)H, J<sub>H,H</sub> = 7.5, 0.8 Hz), 6.74 (d, 2H, CH<sub>Ar</sub> (benzoate ligand), J<sub>H,H</sub> = 0.6 Hz), 6.72 (tm, 1H, Ar(PO)H, J<sub>H,H</sub> = 8.1 Hz), 6.63 (ddd, 1H, Ar(PO)H, J<sub>H,H</sub> = 8.4, 4.3, 0.9 Hz), 5.19 (m, 1H, CH(isopropoxy)), 2.21 (s, 3H, CH<sub>3,para</sub> (benzoate ligand)), 2.18 (s, 6H, CH<sub>3,ortho</sub> (benzoate ligand)), 1.70 (d, 3H,

CH<sub>3</sub>(isopropoxy), J<sub>H,H</sub> = 6.2 Hz), 1.67 (d, 3H, CH<sub>3</sub>(isopropoxy), J<sub>H,H</sub> = 6.1 Hz), 1.18 (d, 3H, CH<sub>3</sub>(TMP), J<sub>H,P</sub> = 18.1 Hz), 1.15 (d, 3H, CH<sub>3</sub>(TMP), J<sub>H,P</sub> = 12.6 Hz), 1.09 (s, 9H, *tert*-butyl(TMP)). <sup>13</sup>C NMR (150 MHz, CD<sub>2</sub>Cl<sub>2</sub>): δ 290.69 (dd, 1C, C(=Ru), J<sub>C,P</sub> = 42.3, 13.6 Hz), 179.32 (d, 1C, C<sub>Ar(PO)</sub>(ORu), J<sub>C,P</sub> = 14.1 Hz), 178.15 (s, 1C, COO (benzoate ligand)), 155.51 (s, 1C, C<sub>Ar(O)</sub>(OR)), 144.25 (s, 1C, C<sub>Ar(O)</sub>(CH=Ru)), 137.96 (s, 1C, C<sub>para</sub> (benzoate ligand)), ~136.3 and 132.8 (2 very br s almost in the baseline, 2C, C<sub>Ar(P)</sub>(ortho)), 136.03 (s, 2C, C<sub>ortho</sub> (benzoate ligand)), 134.76 (s, 1C, CCOO (benzoate ligand)), 133.60 (s, 1C, C<sub>Ar(PO)</sub>(H)), 132.40 (s, 1C, C<sub>Ar(PO)</sub>(H)), 130.54 (s, 1C, C<sub>Ar(P)</sub>(para)), 130.02 (d, 1C, C<sub>Ar(P)</sub>(ipso), J<sub>C,P</sub> = 46.5 Hz), 129.12 (s, 1C, C<sub>Ar(O)</sub>(H)), 129.00 (s, 2C, C<sub>meta</sub> (benzoate ligand)), 128.16 (d, 2C, C<sub>Ar(P)</sub>(meta), J<sub>C,P</sub> = 9.9 Hz), 123.79 (s, 1C, C<sub>Ar(O)</sub>(H)), 122.90 (s, 1C, C<sub>Ar(O)</sub>(H)), 120.47 (d, C<sub>Ar(PO)</sub>(PRu), J<sub>C,P</sub> = 42.5 Hz), 119.41 (d, 1C, C<sub>Ar(PO)</sub>(H), J<sub>C,P</sub> = 9.8 Hz), 117.06 (d, 1C, C<sub>Ar(PO)</sub>(H), J<sub>C,P</sub> = 6.3 Hz), 114.50 (s, 1C, C<sub>Ar(O)</sub>(H)), 77.27 (s, 1C, C<sub>isopropoxy</sub>), 46.64 (d, 1C, C<sub>TMP</sub>, J<sub>C,P</sub> = 23.8 Hz), 37.79 (d, 1C, C<sub>TMP</sub>, J<sub>C,P</sub> = 3.2 Hz), 28.56 (d, 3C, C<sub>TMP</sub>, J<sub>C,P</sub> = 5.0 Hz), 22.15 (s, 1C, C<sub>isopropoxy</sub>), 22.06 (d, 1C, C<sub>TMP</sub>, J<sub>C,P</sub> = 7.5 Hz), 21.66 (d, 1C, C<sub>TMP</sub>, J<sub>C,P</sub> = 2.1 Hz), 21.32 (s, 1C, C<sub>isopropoxy</sub>), 21.20 (s, 1C, CH<sub>3,para</sub> (benzoate ligand)), 20.95 (s, 2C, CH<sub>3,ortho</sub> (benzoate ligand)). <sup>31</sup>P NMR (121 MHz, CD<sub>2</sub>Cl<sub>2</sub>): δ 78.93 (s). Anal. Calcd (%) for C<sub>39</sub>H<sub>47</sub>O<sub>4</sub>PRu (711.84 g/mol): C 65.81, H 6.65. Found: C 65.61, H 6.65.

**Synthesis of Triisopropylbenzoate Complex 10c.** Catalyst **6a** (10 mg, 13.9 μmol) and sodium 2,4,6-triisopropylbenzoate (4.1 mg, 15.3 μmol) in 2 mL of CH<sub>2</sub>Cl<sub>2</sub> were stirred for 2 h at room temperature. The complex was filtered and used without further purification.

<sup>1</sup>H NMR (600 MHz, CD<sub>2</sub>Cl<sub>2</sub>): δ 16.12 (d, 1H, CH(=Ru), J<sub>H,P</sub> = 8.0 Hz), 8.24 (t, 2H, Ar(P)H<sub>ortho</sub>, J<sub>H,H</sub> = 8.5 Hz), 7.92 (td, 1H, Ar(PO)H, J<sub>H,H</sub> = 7.7, 1.5 Hz), 7.59–7.56 (m, 1H, Ar(O)H), 7.55 (td, 1H, Ar(P)H<sub>para</sub>, J<sub>H,H</sub> = 3.6, 1.6 Hz), 7.51 (t, 2H, Ar(P)H<sub>meta</sub>, J<sub>H,H</sub> = 7.6 Hz), 7.23 (dd, 1H, Ar(O)H, J<sub>H,H</sub> = 7.6, 1.6 Hz), 7.18 (d, 1H, Ar(O)H, J<sub>H,H</sub> = 8.4 Hz), 7.14–7.10 (m, 1H, Ar(O)H), 7.01 (td, 1H, Ar(PO)H, J<sub>H,H</sub> = 7.5, 0.8 Hz), 6.87 (s, 2H, CH<sub>Ar</sub> (benzoate ligand)), 6.73 (tm, 1H, Ar(PO)H, J<sub>H,H</sub> = 8.0 Hz), 6.64 (ddd, 1H, Ar(PO)H, J<sub>H,H</sub> = 8.4, 4.4, 0.9 Hz), 5.23 (m, 1H, CH(isopropoxy)), 2.83 (m, 3H, CH<sub>isopropyl,ortho and para</sub> (benzoate ligand)), 1.88 (d, 3H, CH<sub>3</sub>(isopropoxy), J<sub>H,H</sub> = 6.2 Hz), 1.65 (d, 3H, CH<sub>3</sub>(isopropoxy), J<sub>H,H</sub> = 6.0 Hz), 1.23 (d, 3H, CH<sub>3</sub>(TMP), J<sub>H,P</sub> = 11.9 Hz), 1.20 (two d, 6H, CH<sub>3,para</sub> (benzoate ligand), J<sub>H,H</sub> = 6.9 Hz), 1.18 (s, 9H, *tert*-butyl(TMP)), 1.17 (d, 3H, CH<sub>3</sub>(TMP), J<sub>H,P</sub> = 16.1 Hz), 1.12 (d, 6H, CH<sub>3,ortho</sub> (benzoate ligand), J<sub>H,H</sub> = 6.9 Hz), 0.87 (d, 6H, CH<sub>3,ortho</sub> (benzoate ligand), J<sub>H,H</sub> = 6.8 Hz). <sup>13</sup>C NMR (150 MHz, CD<sub>2</sub>Cl<sub>2</sub>): δ 291.85 (d, 1C, C(=Ru), J<sub>C,P</sub> = 12.9 Hz), 179.19 (d, 1C, C<sub>Ar(PO)</sub>(ORu), J<sub>C,P</sub> = 14.2 Hz), 176.64 (s, 1C, COO (benzoate ligand)), 155.21 (s, 1C, C<sub>Ar(O)</sub>(OR)), 148.37 (s, 1C, C<sub>para</sub> (benzoate ligand)), 144.80 (s, 2C, C<sub>ortho</sub> (benzoate ligand)), 144.26 (s, 1C, C<sub>Ar(O)</sub>(CH=Ru)), 136.59 (s, 1C, CCOO (benzoate ligand)), ~136.3 and 132.8 (2 very br s almost in the baseline, 2C, C<sub>Ar(P)</sub>(ortho)), 133.43 (s, 1C, C<sub>Ar(PO)</sub>(H)), 132.56 (s, 1C, C<sub>Ar(PO)</sub>(H)), 130.83 (d, 1C, C<sub>Ar(P)</sub>(para), J<sub>C,P</sub> = 2.2 Hz), 129.31 (s, 1C, C<sub>Ar(O)</sub>(H)), 128.67 (d, 1C, C<sub>Ar(P)</sub>(ipso), J<sub>C,P</sub> = 47.1 Hz), 128.28 (d, 2C, C<sub>Ar(P)</sub>(meta), J<sub>C,P</sub> = 10.1 Hz), 123.91 (s, 1C, C<sub>Ar(O)</sub>(H)), 123.10 (s, 1C, C<sub>Ar(O)</sub>(H)), 120.99 (s, 2C, C<sub>meta</sub> (benzoate ligand)), 120.58 (d, C<sub>Ar(PO)</sub>(PRu), J<sub>C,P</sub> = 43.0 Hz), 119.66 (d, 1C, C<sub>Ar(PO)</sub>(H), J<sub>C,P</sub> = 9.8 Hz), 117.35 (d, 1C, C<sub>Ar(PO)</sub>(H), J<sub>C,P</sub> = 6.3 Hz), 114.56 (s, 1C, C<sub>Ar(O)</sub>(H)), 76.70 (s, 1C, C<sub>isopropoxy</sub>), 46.80 (d, 1C, C<sub>TMP</sub>, J<sub>C,P</sub> = 23.9 Hz), 37.47 (d, 1C, C<sub>TMP</sub>, J<sub>C,P</sub> = 4.6 Hz), 34.82 (s, 1C, CH(CH<sub>3</sub>)<sub>2,para</sub>), 31.22 (s, 2C, CH(CH<sub>3</sub>)<sub>2,ortho</sub>), 28.79 (d, 3C, C<sub>TMP</sub>, J<sub>C,P</sub> = 5.4 Hz), 24.61 (s, 4C, CH(CH<sub>3</sub>)<sub>2,ortho</sub>), 24.35 (s, 2C, CH(CH<sub>3</sub>)<sub>2,para</sub>), 24.33 (s, 1C, CH(CH<sub>3</sub>)<sub>2,para</sub>), 22.67 (s, 1C, C<sub>isopropoxy</sub>), 22.05 (d, 1C, C<sub>TMP</sub>, J<sub>C,P</sub> = 7.2 Hz), 21.10 (s, 1C, C<sub>isopropoxy</sub>), 20.71 (d, 1C, C<sub>TMP</sub>, J<sub>C,P</sub> = 4.0 Hz). <sup>31</sup>P NMR (121 MHz, CD<sub>2</sub>Cl<sub>2</sub>): δ 81.64 (s). Anal. Calcd (%) for C<sub>45</sub>H<sub>59</sub>O<sub>4</sub>PRu (796.00 g/mol): C 67.90, H 7.47. Found: C 67.61, H 7.66.

**Table 1.** Copolymerization Experiments with Catalysts **5a**, **5b**, **6a**, **7–9**, and **10a–c** Carried out at Room Temperature with 150–200 mg of Norbornene (NBE), and 20 equiv of Cyclooctene (COE) with the Reaction Volume Filled up to 20 mL with  $\text{CH}_2\text{Cl}_2^a$

catalyst	X	$t$ [min]	yield [%] <sup>b</sup>	alternating linkages [%] <sup>c</sup>	<i>cis</i> content [%] <sup>d</sup>
<b>5a</b>	Cl–	15	88	97	13
<b>5b</b>	Cl–	30	90	97	13
<b>6a</b>	$\text{CH}_3\text{C}_6\text{H}_4\text{SO}_3-$	40	82	95 (1.3)	25
<b>7</b>	$\text{NO}_3-$	40	31	77 (5.2)	20
<b>8</b>	$\text{CH}_3\text{COO}-$	40	27	92 (2.5)	13
<b>9</b>	$\text{CF}_3\text{COO}-$	40	77	92 (1.7)	18
<b>10a</b>	$\text{C}_6\text{H}_5\text{COO}-$	40	26	90 (1.8)	14
<b>10b</b>	2,4,6-Me <sub>3</sub> C <sub>6</sub> H <sub>2</sub> COO–	40	78	96 (0.7)	14
<b>10c</b>	2,4,6-iPr <sub>3</sub> C <sub>6</sub> H <sub>2</sub> COO–	40	71	96 (0.7)	15

<sup>a</sup>NBE/catalyst ratio was 2000:1. <sup>b</sup>Yields were determined after drying the coagulated copolymer under high vacuum for 2 h (relative to 100% totally alternating copolymer). <sup>c</sup>The percentage of alternating linkages has been determined by integration of the olefinic region of the  $^{13}\text{C}$  NMR spectrum; standard deviation is given in parentheses. <sup>d</sup>The *cis* content was estimated by integration of the CH (CH=CHR) protons on the norbornene terminus of the double bond (see Figures S6 and S8).

## COMPUTATIONAL DETAILS

Geometry optimizations were performed with the Amsterdam Density Functional (ADF) package 2010.02 using the BP86 density functional with an all-electron triple- $\zeta$  quality basis set with added polarization functions (TZP) and an integration accuracy of 5.0. Relativistic effects were treated with the spin-orbit coupled zeroth-order regular approximation (ZORA).<sup>43</sup> For simplicity reasons, a truncated model was used replacing 1,1,2,2-tetramethylpropyl (TMP) with a *tert*-butyl substituent and the benzyldiene with a methyldiene carbene. All structures were fully optimized without constraints and checked with frequency calculations to ensure that they were minima. Optimized geometries and absolute energies are given in the Supporting Information.

## RESULTS

A series of ruthenium catalysts with oxy ligands were synthesized (**7–10**) by direct ligand exchange starting from catalyst **6a** (**5b** in the case of trifluoroacetate ligand) with the corresponding salt. Conversions to the desired complexes were fast, showing complete conversion of the starting material within 2 h.

In screening studies of copolymerization of norbornene and cyclooctene (Table 1) catalysts **7** (the nitrate complex), **8** (the acetate complex), and **10a** (the benzoate complex) gave the desired polymers in low conversions (in the range 26–31%). The lower reactivity exhibited by **7** is concomitant with the highest drop in chemoselectivity for alternating copolymerization (among the catalysts tested). The selectivity dropped from 95–97% alternating units in the copolymer produced with **6a** and **5b** to 77% for nitrate catalyst **7** (Figure 2). A smaller decrease in chemoselectivity is observed in the series of benzoate ligands (Figure 3), going from 96% to 90% alternating units. At a first glance, this drop in selectivity might not appear as significant; however, this drop in selectivity is reproducible (all polymerization results were repeated at least three times; Table 1, standard deviations of polymerization results). Thus, it is apparent that the aforementioned changes are significant and do not result from experimental errors.

The trifluoroacetate catalyst **9**, the trimethylbenzoate catalyst **10b**, and the triisopropylbenzoate catalyst **10c** are intermediate in their performance. The drop in chemoselectivity was especially surprising since we expected the chemoselectivity to be

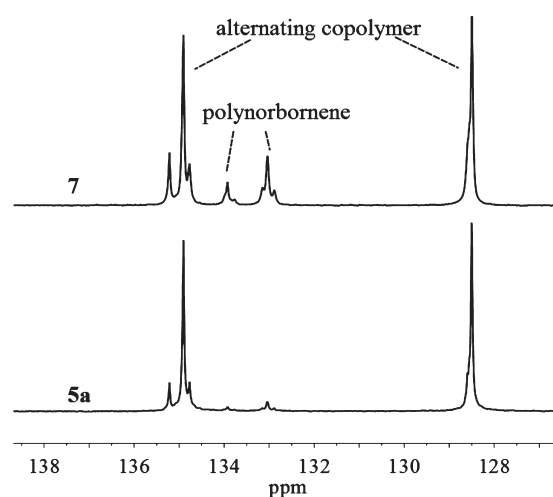


**Figure 2.**  $^{13}\text{C}$  NMR spectra of copolymers produced with catalysts **5a** and **7**.

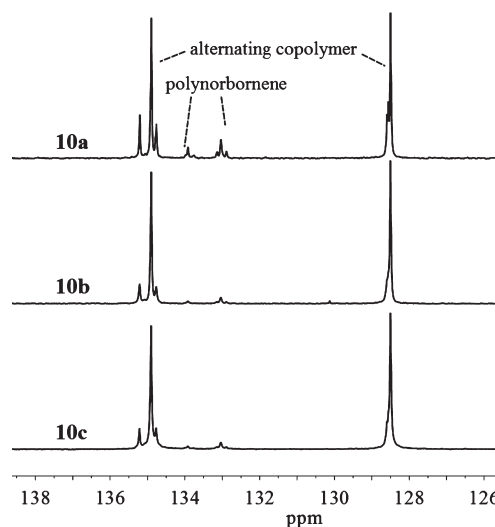


**Figure 3.**  $^{13}\text{C}$  NMR spectra of copolymers produced with catalysts **10a–c**.

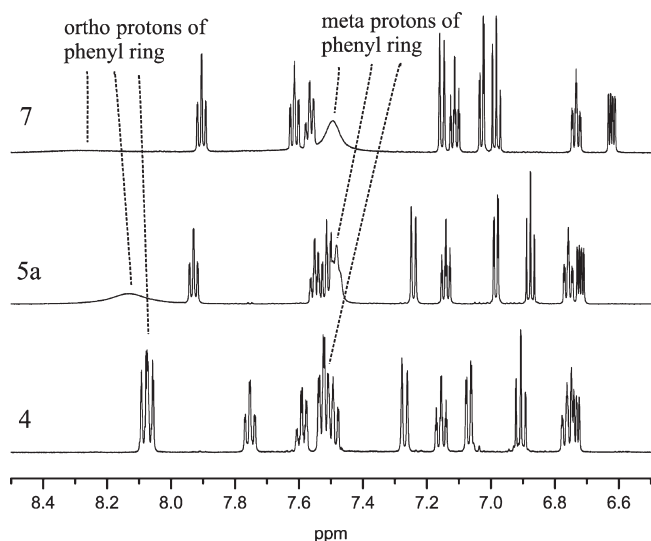


**Figure 4.** Aromatic region of the  $^1\text{H}$  NMR spectra of catalysts 4, 5a, and 7 in  $\text{CD}_2\text{Cl}_2$  at rt (600 MHz).

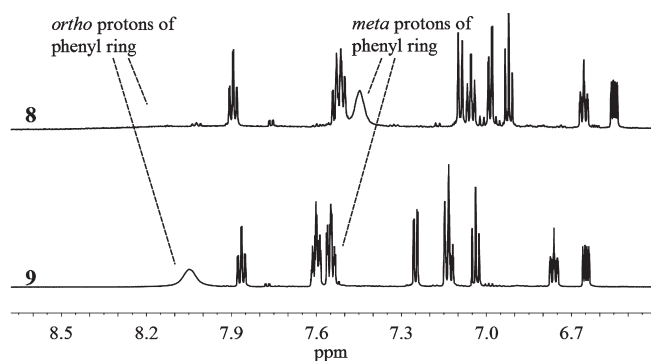


**Figure 5.** Aromatic region of the  $^1\text{H}$  NMR spectra of catalysts 8 and 9 in  $\text{CD}_2\text{Cl}_2$  at rt (600 MHz).

dependent on the size difference of the two substituents on the bidentate phosphine ligand only.

The drop in selectivity and/or reactivity correlates to the observed peak broadening in the  $^1\text{H}$  NMR spectra of the signals for the *ortho* and *meta* protons of the phenyl ring on the bidentate phosphine/phenolate ligand. While the proton signals are well resolved in the case of catalyst 4, the *ortho* and *meta* protons of the phenyl ring are broadened for catalyst 5a (Figure 4). For catalyst 7 the signal for the *meta* protons is further broadened and the signal for the *ortho* protons disappears almost completely in the baseline, which indicates that rotation of the phenyl ring is slow, presumably due to steric hindrance. A similar behavior can be observed for the *ortho* and *meta* protons of the  $^1\text{H}$  NMR spectra of 8 and 9 (Figure 5) and 10a–c (Figure 6). Furthermore, broadening of *ortho* and *meta* carbon signals is seen in the  $^{13}\text{C}$  NMR spectra (see Figures S1, S2, and S3), and no cross-peak is seen between the *ortho* protons and *ortho* carbons of the phenyl ring in the HSQC of complex 7 in  $\text{CD}_2\text{Cl}_2$  (see Figure S13).

Crystal structures of the catalyst complexes give us additional information and help connect catalyst structure to performance (see Table 2). For the ruthenium catalyst with a nitrate ligand (7) (Figure 7) a hexacoordinated complex is formed by a chelating

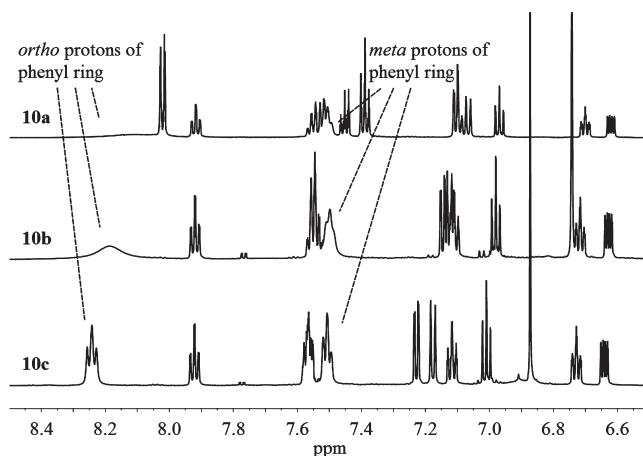


**Figure 6.** Aromatic region of the  $^1\text{H}$  NMR spectra of catalysts 10a–c in  $\text{CD}_2\text{Cl}_2$  at rt (600 MHz).

**Table 2.** Comparison of the Most Significant Structural Parameters for Chelating Interactions in Complexes 4, 5a, 7, 9, 10a,b, and Buchmeiser's Structure 14<sup>32</sup>

complex	Ru–O <sub>short</sub> [Å]	Ru–O <sub>long</sub> [Å]	O–Ru–O [deg]	O–C–O or O–N–O [deg]	Ru–O–N or Ru–O–C [deg]
4			153.13 (8)		
5a			158.68 (10)		
7	2.128 (2)	2.358 (2)	163.22 (9)	114.82 (2)	98.89 (17)
9	2.068 (2)	3.385 (2)	160.42 (9)	131.00 (3)	126.95 (2)
10a	2.142 (2)	2.333 (2)	164.75 (3)	119.79 (3)	93.43 (10)
10b	2.115 (2)	2.406 (2)	168.52 (9)	123.75 (3)	97.85 (19)
14 <sub>chelating</sub>	2.094	2.493		124.55	98.06
14 <sub>nonchelating</sub>	2.022	3.430		130.59	130.87

interaction with a second oxygen atom of the nitrate ligand (Ru–O34 and Ru–O36 distances are 2.128(2) and 2.358(2) Å, respectively). The angle O14–Ru1–O34 (163.22(9)°) is significantly larger than the corresponding angles for the ruthenium catalyst with a chloride ligand (4 (153.13(8)°, Figure S4) and 5a (158.68(10)°, Figure S5)), as a result of the additional chelating interaction. The opening of this angle has an effect on the selectivity: it pushes the whole phosphine ligand closer to the carbene and constrains the space of the phenyl substituent, thereby leading to its hindered rotations, which is the presumed origin of the broader signals in the NMR spectra. The same increased steric encumbrance that hinders the phenyl group rotation would lessen the energetic difference between the two diastereomeric carbenes in the catalytic cycle. A reduced energy difference would manifest itself as a reduced chemoselectivity between norbornene and cyclooctene in the alternating copolymerization, as we have observed. This hypothesis was checked by quantum chemical calculations (Figure 8). Indeed, whereas the energetic difference (ADF–BP86/ZORA–TZP) between the two diastereomeric carbene states for the truncated *tert*-butyl model is 3.4 kcal/mol with a chloride substituent (C1 and C2),<sup>24</sup> the value decreases to 2.7 kcal/mol with a nitrate ligand (N1 and N2). This is due to a stronger chelating interaction of the nitrate ligand (by 0.7 kcal/mol) when the methyldiene carbene is on the side of the *tert*-butyl group (N2). The effect is not very

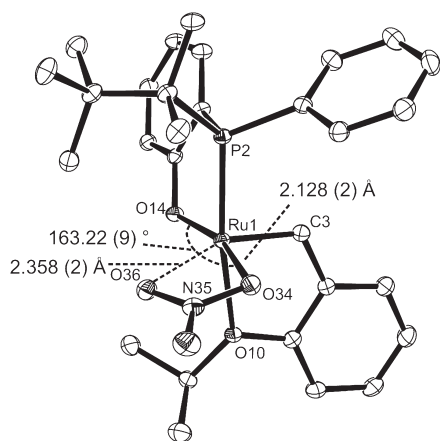


**Figure 7.** Crystal structure of complex **7** (ORTEP plot, 30% probability ellipsoids). Hydrogen atoms are omitted for clarity. Selected distances (Å) and angles (deg): Ru1–C3 1.856(3), Ru1–O14 1.988(2), Ru1–P2 2.2404(8), Ru1–O10 2.278(2), C3–Ru1–O14 100.00(12), C3–Ru1–O34 95.45(11), C3–Ru1–P2 89.69(10), O14–Ru1–P2 84.21(6), O34–Ru1–P2 102.47(7), C3–Ru1–O10 79.75(11), O14–Ru1–O10 89.28(8), O34–Ru1–O10 87.06(8), P2–Ru1–O10 166.47(6), C3–Ru1–O36 150.25(11), O14–Ru1–O36 106.29(8), O34–Ru1–O36 57.17(8), P2–Ru1–O36 106.38(6), O10–Ru1–O36 86.82(8).

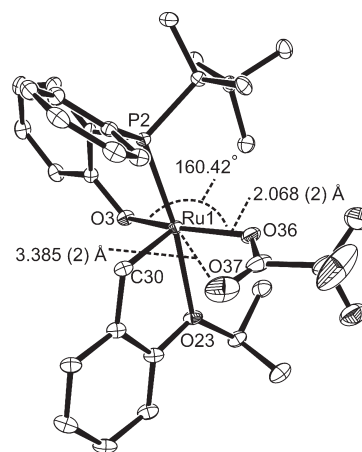
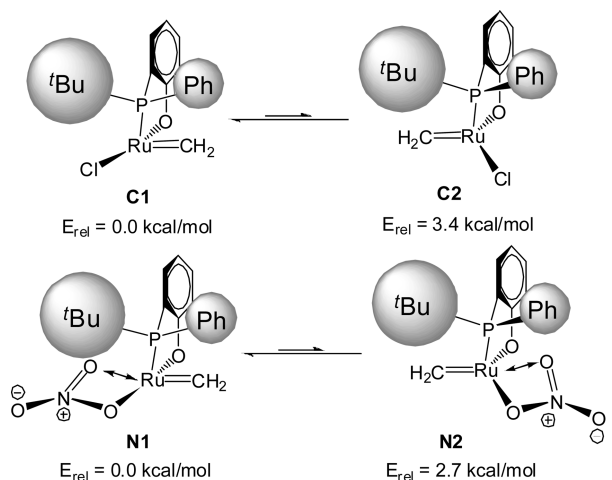


**Figure 9.** Crystal structure of complex **9** (ORTEP plot, 30% probability ellipsoids). Hydrogen atoms are omitted for clarity. Selected distances (Å) and angles (deg): Ru1–C30 1.838(3), Ru1–O3 2.0018(18), Ru1–P2 2.2374(7), Ru1–O23 2.2760(19), C30–Ru1–O3 98.09(10), C30–Ru1–O36 99.68(10), C30–Ru1–P2 95.64(9), O3–Ru1–P2 84.65(6), O36–Ru1–P2 101.65(6), C30–Ru1–O23 79.49(10), O3–Ru1–O23 89.21(8), O36–Ru1–O23 86.03(8).



higher steric energy, because the carbene is on the side of the larger substituent but stronger chelation of the nitrate ligand.

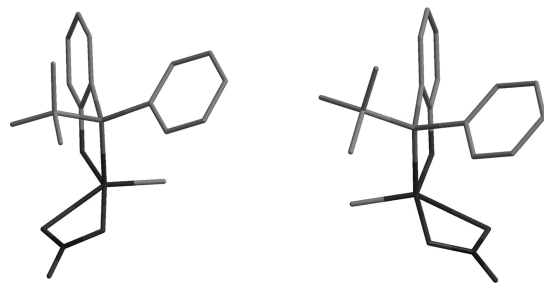


**Figure 8.** Explanation of the lower chemoselectivity reached with catalyst **7** versus **5a**. The nitrate chelation counteracts the steric bulk of the two substituents on the phosphorus ligand. Calculated structures for the nitrate complex are shown at the bottom; hydrogen atoms are omitted for clarity.

pronounced but large enough to produce considerable amounts of polynorbornene linkages during copolymerization of NBE with COE. Gel permeation chromatography (GPC analysis) of the obtained copolymers shows that the sequences of polynorbornene produced are part of the same chain as alternating linkages, which is to be expected from the reaction mechanism (tables in SI). Calculations were done in accordance and agreement with our previous reports, in which a combined experimental and computational investigation indicated that the origin of chemoselectivity in our system is attributable to diastereomeric site control.<sup>24</sup>

Catalyst **9** (Figure 9) does not show a chelation of the trifluoroacetate ligand, with the Ru–O37 bond length of 3.385(2) Å. The O3–Ru1–O36 angle, at 160.42(9)°, is slightly larger than the corresponding angle for catalyst **5a** (158.68(10)°). This effect can be explained by the larger size of the anion itself. Still, the angle is smaller than in the case of complex **7**. The fact that the trifluoroacetate ligand does not show chelation, while the acetate one does, could be explained by both steric and electronic factors (CF<sub>3</sub> is strongly electron-withdrawing). One may venture to suggest that chelation influences reactivity more than it does chemoselectivity (Table 1). The lower activity of the catalysts **7**, **8**, and **10a** could be explained by the stabilizing effect of chelating ligands on the Ru center.

A less pronounced chelation is seen in the crystal structure of **10b** (Figure 11) as compared to **10a** (Figure 10). The difference between Ru–O bonds in **10a** (2.142(2) and 2.333(2) Å) is smaller compared to those in **10b** (2.115(2) and 2.406(2) Å), which indicates stronger chelation in the case of the former, most probably due to sterics. Although the angle O9–Ru–O45 in **10b** (168.52(9)°) is significantly larger than the corresponding angle in **10a** (164.75(3)°), less broadening of the NMR signals was observed. Due to the weaker chelation in complex **10b**, there is a better chance of opening of the chelate ring, allowing for a more facile rotation in solution and observing it on the NMR time scale. It can also be noted that the *cis* content of obtained polymers with benzoate catalysts is rather low compared to sulfonate ones (14–15% for catalysts **10a–c**), which may be

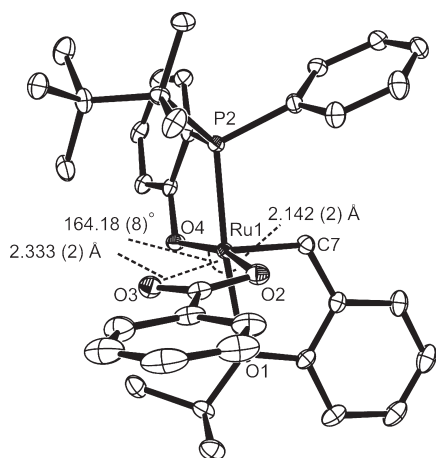


**Figure 10.** Crystal structure of complex **10a** (ORTEP plot, 30% probability ellipsoids). Hydrogen atoms are omitted for clarity. Selected distances (Å) and angles (deg): Ru(1)–C(7) 1.845(3), Ru(1)–O(4) 2.0046(19), Ru(1)–P(2) 2.2358(7), Ru(1)–O(1) 2.2643(19), C(7)–Ru(1)–O(4) 100.64(10), C(7)–Ru(1)–O(2) 93.99(10), C(7)–Ru(1)–P(2) 91.38(9), O(4)–Ru(1)–P(2) 84.45(6), O(2)–Ru(1)–P(2) 101.29(6), C(7)–Ru(1)–O(1) 79.66(10), O(4)–Ru(1)–O(1) 89.65(7), O(2)–Ru(1)–O(1) 87.08(7), P(2)–Ru(1)–O(1) 168.20(5), C(7)–Ru(1)–O(3) 150.45(10), O(4)–Ru(1)–O(3) 106.39(7), O(2)–Ru(1)–O(3) 58.10(7), P(2)–Ru(1)–O(3) 102.79(5), O(1)–Ru(1)–O(3) 88.66(7).

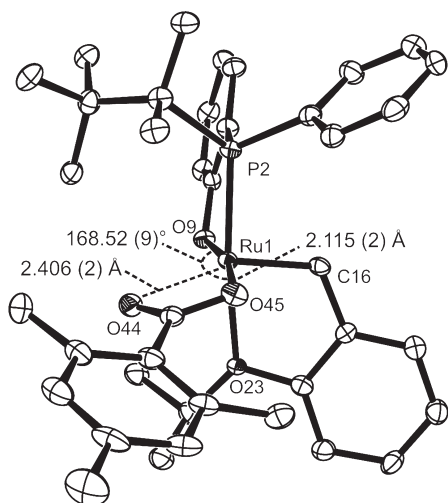


**Figure 11.** Crystal structure of complex **10b** (ORTEP plot, 30% probability ellipsoids). Hydrogen atoms are omitted for clarity. Selected distances (Å) and angles (deg): Ru(1)–C(16) 1.852(3), Ru(1)–O(9) 2.019(2), Ru(1)–P(2) 2.2321(9), Ru(1)–O(23) 2.239(2), C(16)–Ru(1)–O(9) 101.20(11), C(16)–Ru(1)–O(45) 89.05(11), C(16)–Ru(1)–P(2) 92.75(12), O(9)–Ru(1)–P(2) 84.35(7), O(45)–Ru(1)–P(2) 100.44(7), C(16)–Ru(1)–O(23) 80.76(13), O(9)–Ru(1)–O(23) 89.23(9), O(45)–Ru(1)–O(23) 87.33(9), P(2)–Ru(1)–O(23) 169.85(6), C(16)–Ru(1)–O(44) 142.27(10), O(9)–Ru(1)–O(44) 111.44(9), O(45)–Ru(1)–O(44) 57.19(9), P(2)–Ru(1)–O(44) 108.39(6), O(23)–Ru(1)–O(44) 81.28(8).

explained by the fact that the oxygen atoms of the  $\text{SO}_3$  group (in contrast to a carboxylate) are pointing more toward the active site, as has been structurally proven by X-ray crystallography.<sup>23</sup> The incoming norbornene would then coordinate in such a way to avoid steric interaction with the bridgehead.

## DISCUSSION

On our way toward the development of a chemo- and stereoselective ruthenium-based catalyst for the alternating copolymerization of norbornene and cyclooctene, which is based on two diastereomeric carbene states in the catalytic cycle,<sup>18–24</sup> we uncovered interesting steric features, which, in hindsight, allow for a more detailed understanding of this system.

The solid-state structure of our original prototype **3** was somewhat unexpected since the carbene was on the side of the more bulky *tert*-butyl group rather than below the smaller phenyl ring, an effect that was caused by a C–H agostic interaction between one cyclohexyl ring and the ruthenium center (Chart 1). The agostic interaction rendered the cyclohexyl ring sterically more demanding than the carbene.<sup>22</sup>

We then improved our system by introducing a Hoveyda-type<sup>13,14,46–49</sup> carbene unit (**4**),<sup>22</sup> which shows the reverse and expected configuration around the metal center. In this complex the chelating carbene unit with the hydrogen atom pointing “up” (toward the substituents on the phosphorus) is on the side of the smaller phenyl ring. This was followed by the optimization of the bidentate phosphine/phenolate ligand to yield a totally chemo-selective AROMP catalyst (**5a**, **5b**).<sup>24</sup> Other examples of AROMP catalysts can be found in the literature.<sup>50–56</sup>

Replacement of the chloride anion in **5b** with various sulfonates (**11a–d**) of increasing steric bulk allowed us to influence the *cis/trans* ratio of the produced copolymer, leaving the chemoselectivity unchanged (**6a–d**).<sup>23</sup> Schrock and Hoveyda also published *Z*-selective molybdenum catalysts.<sup>57,58</sup>

From these results, we considered that chemo- and stereoselectivity in ruthenium-catalyzed olefin metathesis have their origin in defined steric parameters that we have been optimizing by careful tuning of the substituents on the ligands.<sup>22–24</sup> Reactivity, on the other hand, is usually believed to be determined primarily by electronic properties of ligands. A more electron-donating NHC ligand<sup>44</sup> (i.e., the second-generation Grubbs catalyst **2**) in general gives a more reactive catalyst compared to the first-generation Grubbs systems featuring phosphines (**1**). In the case of the phosphine ligands larger and more electron-donating ones are favored.<sup>40</sup> Among the anions, chloride-containing catalysts exhibit the highest activity, albeit at the expense of the possibility for steric modifications that would allow tuning of the *cis/trans* ratio.<sup>40</sup> The aforementioned strongly electron-withdrawing sulfonate ligand-containing complexes **6a–d** present an alternative to the chloride. However, despite the possibility of tuning the *cis/trans* ratio, they already induce a significantly diminished reactivity as compared to the parent complex **5b**.<sup>23</sup> This stands in contrast to the results of a computational study of Straub,<sup>45</sup> where calculations for NHC–Ru complexes predicted sulfonates to be equally efficient or even superior as compared to chloride.

Further alternatives to the chloride ligand are carboxylate ligands, again due to their electron-withdrawing character. Recently Ru-carboxylate olefin metathesis catalysts were prepared as an alternative for Ru-chlorides (Figure 1).<sup>25–39</sup> Numerous supported (i.e., **13**) and unsupported (i.e., **14**, **15**) Grubbs-, Hoveyda–Grubbs-, or Grubbs–Herrmann-type catalysts have been reported. Fluorinated carboxylate (e.g., trifluoroacetate, pentafluoropropionate, pentafluorobenzoate) ligands are usually used because of their strong electron-withdrawing effect, which is expected to produce high activities in metathesis reactions. Examples of chelate effects are reported as well, giving catalysts with low (**15**) or high reactivities (**16**, see discussion below), although comparisons are difficult, as multiple factors are varied at the same time.

Blechert and Buchmeiser, for example, have used triflate and carboxylate anions with electron-poor alkyl chains (for example trifluoroacetate).<sup>25–33</sup> Buchmeiser and co-workers disclosed one crystal structure with two trifluoroacetate anions, which, in contrast to our example, shows a possible chelating interaction involving one of the anions. One could hypothesize that this could also have an impact on selectivity (catalyst **14**, Figure 1).<sup>32</sup> In that instance, the chelating trifluoroacetate anion shows Ru–O distances of 2.094 and 2.493 Å. The latter distance is longer as compared to nitrate complex **7** or benzoate complexes **10a,b**, indicating that nitrate and benzoate form stronger chelates (Table 2). Evidence that there is, in fact, a chelating interaction in Buchmeiser's complex is given by the larger O–C–O angle of the second, nonchelating trifluoroacetate anion (130.59° compared to 124.55° for the chelating one) and from the very small Ru–O–C angle of the chelating one (98.06°).

To compare nitrate and trifluoroacetate anions directly, one might consider the following literature: Ruthenium nitrate complexes  $[\text{Ru}(\text{NO}_3)_x(\text{O}_2\text{CCF}_3)_{2-x}(\text{CO})(\text{PPh}_3)_2]$  have been reported by Robinson et al. for the catalytic dehydrogenation of primary and secondary alcohols to aldehydes and ketones, respectively. The bis-trifluoroacetate complex shows much greater catalytic efficiency relative to the bis-nitrate complex. In the latter complex the alcohol has to compete with the nitrate anion, a stronger chelating ligand than the trifluoroacetate anion, in order to enter the coordination sphere.<sup>59</sup>

For our complexes, we can conclude from the crystallographic data (Table 2) that the nitrate ligand in complex **7** is the strongest chelating ligand among the oxyanions examined in this paper. Important structural features are Ru–O distances and O–C–O and Ru–O–C angles. In the nitrate complex, the O–N–O angle (114.82(2)°) is significantly smaller compared to others: 131.00(3)°, 119.79(3)°, and 123.75°(3) for **9**, **10a**, and **10b**, respectively. Here we can also see the agreement with the angles for chelating and nonchelating ligands in Buchmeiser's complex (123.75(3)° in **10a** compared to 124.55° for chelating and 131.00(3)° in **9** compared to 130.59° for nonchelating ligand in catalyst **14**). Comparing the Ru–O–N angle with the Ru–O–C angle, the same effect can be seen: 98.89(17)° in the nitrate complex compared to 93.43(10)° and 97.85 (19)° in **10a** and **10b**, which are significantly smaller compared to the 126.95(2)° of complex **9**. The conclusion that the nitrate ligand is the strongest chelating agent is supported by the polymerization results, since nitrate complex **7** gives the biggest drop in chemoselectivity (77%).

The results shown in this paper might be discussed considering  $\text{p}K_a$  values of the conjugate acids of the anionic ligands. From the literature,<sup>60,61</sup> the order of increasing  $\text{p}K_a$ 's would be as follows:  $\text{Cl}^- < \text{NO}_3^- < \text{CF}_3\text{COO}^- < \text{C}_6\text{H}_5\text{COO}^- \sim \text{Me}_3\text{C}_6\text{H}_5\text{COO}^- < \text{CH}_3\text{COO}^-$ . Accordingly, one would expect the following reactivity trend (**7** > **9** > **8**) and that reactivities for benzoate complexes **10a–c** are similar. However, this assumption holds only for the comparison of acetate and trifluoroacetate, but not for the other cases. Nitrate complex **7** is more than 2-fold less reactive than the trifluoroacetate complex (**9**), while benzoate complex **10a** is as much as 3-fold less reactive than the trimethyl and triisopropylbenzoate complexes **10b** and **10c**. Again, we attribute this behavior to the chelating effect of nitrate and benzoate ligands, which stabilize the Ru center, rendering it less reactive.

In other words, the more electron-rich Ru center has a lower tendency for olefin binding, since the chelating interaction would actually favor its dissociation. A similar chelate effect has been

observed by the Grubbs group for complex **16**,<sup>36</sup> where interaction of one of the *ortho* fluorine substituents on the NHC ligand with the metal center promotes phosphine dissociation, hence yielding a more active catalyst.

Regarding the crystal structures, one should take into consideration that the real situation in solution might be different than in the solid state. The NMR data indicate the dynamics of the molecule, i.e., in real time the constrained space for the phenyl substituent. Upon comparison of the NMR data of the complexes to the polymerization results, it can be concluded that a significant broadening of the phenyl signals also correlates with diminished chemoselectivity and/or reactivity. We attribute the broadening of NMR signals to hindered phenyl rotation due to structural distortions induced by chelation by the oxyanion ligands. Most likely this involves a fluctuating behavior of the chelating anion in solution. Rotation of the phenyl ring will be the faster, the easier the anion can switch from a bidentate to a monodentate coordination mode. The same increased steric hindrance of the phenyl rotation diminishes the steric difference between the two diastereomeric sites in the catalytic cycle, thus diminishing the selectivity for alternating copolymerization.

## CONCLUSION

We have shown another interesting structural effect caused by chelating ligands that can reduce selectivity and/or reactivity in AROMP of norbornene and cyclooctene. Given the recent interest in more versatile substitutes for chloride ligands in metathesis catalysts, one should consider the possibility that a given oxyanion substitute for chloride could chelate and adversely affect the desired reactivity or selectivity. The NMR and X-ray-based indicators should give advanced guidance for the cases where one might expect these adverse effects.

## ASSOCIATED CONTENT

**S** Supporting Information. Comparison of <sup>13</sup>C NMR spectra of complexes **5a**, **7–9**, and **10a–c** (Figures S1, S2, and S3), crystal structures of complexes **4** and **5a** (Figures S4 and S5), crystallographic data for complexes **7**, **8**, and **10a,b** (Table S1–4), <sup>1</sup>H NMR spectra of copolymers (Figures S6 and S8), <sup>13</sup>C NMR spectra of copolymers with catalysts **8** and **9** (Figure S7), <sup>1</sup>H and <sup>13</sup>C NMR spectra of complexes **5a**, **7–9**, and **10a–c** (Figures S9–S12, S14–S23), HSQC experiment of complex **7** (Figure S13), details of the DFT calculations, and GPC results of polymers obtained with catalysts **7** and **10b**. This material is available free of charge via the Internet at <http://pubs.acs.org>.

## AUTHOR INFORMATION

### Corresponding Author

\*Tel: (+41) 44 632 2898. Fax: (+41) 44 632 1280. E-mail: peter.chen@org.chem.ethz.ch.

## ACKNOWLEDGMENT

We thank Dr. Bernd Schweizer and Dr. Michael Solar from the X-ray crystallographic service of the ETH and Dr. Philip Zumbrennen and Dr. Rainer Frankensteiner from the NMR service of the Laboratorium für Organische Chemie (ETH) for performing the corresponding experiments.

## REFERENCES

- (1) Chauvin, Y. *Angew. Chem., Int. Ed.* **2006**, *45*, 3741–3747.
- (2) Schrock, R. R. *Angew. Chem., Int. Ed.* **2006**, *45*, 3748–3759.
- (3) Grubbs, R. H. *Angew. Chem., Int. Ed.* **2006**, *45*, 3760–3765.
- (4) Hoveyda, A. H.; Zhugralin, A. R. *Nature* **2007**, *450*, 243–251.
- (5) Casey, C. P. *J. Chem. Educ.* **2006**, *83*, 192–195.
- (6) Trnka, T. M.; Grubbs, R. H. *Acc. Chem. Res.* **2001**, *34*, 18–29.
- (7) Astruc, D. *New J. Chem.* **2005**, *29*, 42–56.
- (8) Katz, T. J. *New J. Chem.* **2006**, *30*, 1844–1847.
- (9) Deshmukh, P. H.; Blechert, S. *Dalton Trans.* **2007**, 2479–2491.
- (10) Vougioukalakis, G. C.; Grubbs, R. H. *Chem. Rev.* **2010**, *110*, 1746–1787.
- (11) Scholl, M.; Trnka, T. M.; Morgan, J. P.; Grubbs, R. H. *Tetrahedron Lett.* **1999**, *40*, 2247–2250.
- (12) Bielawski, C. W.; Grubbs, R. H. *Angew. Chem.* **2000**, *112*, 3025–3028.
- (13) Kingsbury, J. S.; Harrity, J. P. A.; Bonitatebus, P. J., Jr.; Hoveyda, A. H. *J. Am. Chem. Soc.* **1999**, *121*, 791–799.
- (14) Garber, S. B.; Kingsbury, J. S.; Gray, B. L.; Hoveyda, A. H. *J. Am. Chem. Soc.* **2000**, *122*, 8168–8179.
- (15) Conrad, J. C.; Amoroso, D.; Czechura, P.; Yap, G. P. A.; Fogg, D. E. *Organometallics* **2003**, *22*, 3634–3636.
- (16) Monfette, S.; Fogg, D. E. *Organometallics* **2006**, *25*, 1940–1944.
- (17) Conrad, J. C.; Parnas, H. H.; Snelgrove, J. L.; Fogg, D. E. *J. Am. Chem. Soc.* **2005**, *127*, 11882–11883.
- (18) Adlhart, C.; Hinderling, C.; Baumann, H.; Chen, P. *J. Am. Chem. Soc.* **2000**, *122*, 8204–8214.
- (19) Adlhart, C.; Chen, P. *J. Am. Chem. Soc.* **2004**, *126*, 3496–3510.
- (20) Adlhart, C.; Chen, P. *Angew. Chem., Int. Ed.* **2002**, *41*, 4484–4487.
- (21) Bornand, M.; Chen, P. *Angew. Chem., Int. Ed.* **2005**, *44*, 7909–7911.
- (22) Bornand, M.; Torker, S.; Chen, P. *Organometallics* **2007**, *26*, 3585–3596.
- (23) Torker, S.; Mueller, A.; Chen, P. *Angew. Chem., Int. Ed.* **2010**, *49*, 3762–3766.
- (24) Torker, S.; Mueller, A.; Sigrist, R.; Chen, P. *Organometallics* **2010**, *29*, 2735–2751.
- (25) Krause, J. O.; Lubbad, S.; Nuyken, O.; Buchmeiser, M. R. *Adv. Synth. Catal.* **2003**, *345*, 996–1004.
- (26) Krause, J. O.; Lubbad, S. H.; Nuyken, O.; Buchmeiser, M. R. *Macromol. Rapid Commun.* **2003**, *24*, 875–878.
- (27) Krause, J. O.; Zarka, M., T.; Anders, U.; Weberskirch, R.; Nuyken, O.; Buchmeiser, M. R. *Angew. Chem., Int. Ed.* **2003**, *42*, 5965–5969.
- (28) Krause, J. O.; Nuyken, O.; Wurst, K.; Buchmeiser, M. R. *Chem.—Eur. J.* **2004**, *10*, 777–784.
- (29) Yang, L.; Mayr, M.; Wurst, K.; Buchmeiser, M. R. *Chem.—Eur. J.* **2004**, *10*, 5761–5770.
- (30) Halbach, T. S.; Mix, S.; Fischer, D.; Maechling, S.; Krause, J. O.; Sievers, C.; Blechert, S.; Nuyken, O.; Buchmeiser, M. R. *J. Org. Chem.* **2005**, *70*, 4687–4694.
- (31) Vehlow, K.; Maechling, S.; Köhler, K.; Blechert, S. *Tetrahedron Lett.* **2006**, *47*, 8617–8620.
- (32) Kumar, P. S.; Wurst, K.; Buchmeiser, M. R. *J. Am. Chem. Soc.* **2009**, *131*, 387–395.
- (33) Kumar, P. S.; Wurst, K.; Buchmeiser, M. R. *Organometallics* **2009**, *28*, 1785–1790.
- (34) Gawin, R.; Czarnecka, P.; Grela, K. *Tetrahedron* **2010**, *66*, 1051–1056.
- (35) Gawin, R.; Makal, A.; Wozniak, K.; Mauduit, M.; Grela, K. *Angew. Chem., Int. Ed.* **2007**, *46*, 7206–7209.
- (36) Ritter, T.; Day, M. W.; Grubbs, R. H. *J. Am. Chem. Soc.* **2006**, *128*, 11768–11769.
- (37) Nieczypor, P.; Buchowitz, W.; Meester, W. J. N.; Rutjes, F. P. J. T.; Mol, J. C. *Tetrahedron Lett.* **2001**, *42*, 7103–7105.
- (38) Samec, J. S. M.; Grubbs, R. H. *Chem. Commun.* **2007**, 2826–2828.
- (39) Samec, J. S. M.; Grubbs, R. H. *Chem.—Eur. J.* **2008**, *14*, 2686–2692.
- (40) Sanford, M. S.; Love, J. A.; Grubbs, R. H. *J. Am. Chem. Soc.* **2001**, *123*, 6543–6554.
- (41) Seiders, T. J.; Ward, D. W.; Grubbs, R. H. *Org. Lett.* **2001**, *3*, 3225–3228.
- (42) Dias, E. L.; Nguyen, S. T.; Grubbs, R. H. *J. Am. Chem. Soc.* **1997**, *119*, 3887–3897.
- (43) (a) te Velde, G.; Bickelhaupt, F. M.; Baerends, E. J.; Fonseca Guerra, C.; van Gisbergen, S. J. A.; Snijders, J. G.; Ziegler, T. *Chemistry with ADF. J. Comput. Chem.* **2001**, *22*, 931–967. (b) Fonseca Guerra, C.; Snijders, J. G.; te Velde, G.; Baerends, E. J. *Theor. Chem. Acc.* **1998**, *99*, 391–403. (c) *ADF2004.01*; SCM, Theoretical Chemistry, Vrije Universiteit: Amsterdam, The Netherlands, <http://www.scm.com>.
- (44) Diez-Gonzalez, S.; Nolan, S. P. *Coord. Chem. Rev.* **2007**, *251*, 874–883.
- (45) Straub, B. F. *Adv. Synth. Catal.* **2007**, *349*, 204–214.
- (46) Van Veldhuizen, J. J.; Gillingham, D. G.; Garber, S. B.; Kataoka, O.; Hoveyda, A. H. *J. Am. Chem. Soc.* **2003**, *125*, 12502–12508.
- (47) Van Veldhuizen, J. J.; Garber, S. B.; Kingsbury, J. S.; Hoveyda, A. H. *J. Am. Chem. Soc.* **2002**, *124*, 4954–4955.
- (48) Gillingham, D. G.; Kataoka, O.; Garber, S. B.; Hoveyda, A. H. *J. Am. Chem. Soc.* **2004**, *126*, 12288–12290.
- (49) Hoveyda, A. H.; Gillingham, D. G.; Van Veldhuizen, J. J.; Kataoka, O.; Garber, S. B.; Kingsbury, J. S.; Harrity, J. P. A. *Org. Biomol. Chem.* **2004**, *2*, 8–23.
- (50) Vehlow, K.; Wang, D.; Buchmeiser, M. R.; Blechert, S. *Angew. Chem., Int. Ed.* **2008**, *47*, 2615–2618.
- (51) Lichtenheldt, M.; Wang, D.; Vehlow, K.; Reinhardt, I.; Kühnel, C.; Decker, U.; Blechert, S.; Buchmeiser, M. R. *Chem.—Eur. J.* **2009**, *15*, 9451–9457.
- (52) Al Samak, B.; Amir-Ebrahimi, V.; Corry, D. G.; Hamilton, J. G.; Rigby, S.; Rooney, J. J.; Thompson, J. M. *J. Mol. Catal. A: Chem.* **2000**, *160*, 13–21.
- (53) Amir-Ebrahimi, V.; Rooney, J. J. *J. Mol. Catal. A: Chem.* **2004**, *208*, 115–121.
- (54) Hamilton, J. G.; Ivin, K. J.; Rooney, J. J.; Waring, L. C. *J. Chem. Soc., Chem. Commun.* **1983**, 159–161.
- (55) Ilker, M. F.; Coughlin, E. B. *Macromolecules* **2002**, *35*, 54–58.
- (56) Song, A. R.; Parker, K. A.; Sampson, N. S. *J. Am. Chem. Soc.* **2009**, *131*, 3444–3445.
- (57) Flook, M. M.; Jiang, A. J.; Schrock, R. R.; Müller, P.; Hoveyda, A. H. *J. Am. Chem. Soc.* **2009**, *131*, 7962–7963.
- (58) Flook, M. M.; Ng, V. W. L.; Schrock, R. R. *J. Am. Chem. Soc.* **2011**, *133*, 1784–1786.
- (59) Critchlow, P. B.; Robinson, S. D. *Inorg. Chem.* **1978**, *17*, 1902–1908.
- (60) Bordwell, F. G. *Acc. Chem. Res.* **1988**, *21*, 456–463.
- (61) Jover, J.; Bosque, R.; Sales, J. *QSAR Comb. Sci.* **2008**, *27*, 563–581.